Mater. Res. Soc. Symp. Proc. Vol. 1267 © 2010 Materials Research Society 1267-DD08-12

Colloidal nanostructures as building blocks for macroscopic thermoelectric materials with electron-crystal phonon-glass properties

Marcus Scheele[1], Niels Oeschler[2], Katrin Meier[2], Andreas Kornowski[1], Christian Klinke[1], and Horst Weller[1]

[1]University of Hamburg, Institute of Physical Chemistry, Grindelallee 117, 20146 Hamburg, Germany
[2]Max Planck Institute of Chemical Physics of Solids, Noethnitzer Strasse 40, 01187 Dresden, Germany

ABSTRACT

We demonstrate the shape- and size-controlled synthesis of colloidal ~10 nm bismuth telluride nanoparticles stabilized by organic ligands in solution. Post-synthetic ligand exchange with oleic acid allows for a quick and simple ligand removal by consecutive washing with basic ammonia solution. Mild spark plasma sintering yields a macroscopic nanostructured bulk solid with nanograins unaltered in size and shape. We present the full thermoelectric characterization with an emphasis on the thermal properties of this material. It will be shown that thus prepared nanostructured bulk solids possess significantly altered physical properties typical for materials with high surface-to-volume-ratios. These alterations have the potential to lead to improved thermoelectric performances benefiting from their phonon-glass electron-crystal behavior.

INTRODUCTION

Fabrication methods of nanostructured bulk solids can generally be divided into top-down and bottom-up techniques. As an example for the former, ball-milling of macroscopic ingots to nanograins followed by hot-pressing has led to remarkable improvements in the thermoelectric figure of merit (ZT) of these materials [1]. Bottom-up techniques such as hydrothermal [2] and wet-chemical methods [3] have been exploited as an alternative to nanograin synthesis followed by sintering to macroscopic pellets. To control the rate of crystal grain growth and stabilize the highly energetic surfaces of small nanograins, long-chained coordinating organic molecules such as thiols, carboxylic acids, or amines are added to the reaction mixture. These molecules, referred to in the following as ligands, play a key role in bottom-up synthesis and allow excellent control over shape, size, and size distribution of the nanograins. Since thermoelectric properties are known to depend strongly on these parameters for grains on the nanoscale [4], bottom-up nanograin synthesis offers exciting possibilities to designing high-performance thermoelectric materials. PbSe nanograins obtained by wet-chemical synthesis were reported to show a remarkable increase in thermopower attributed to sharp spikes in the density of states [5]. However, a major draw-back in previous works was the often low electric conductivity in the final nanostructured bulk solids. This can immediately be understood when imagining the two component structure of individual nanograins obtained by wet-chemical synthesis: The inorganic, highly conductive nanograin core and the organic, insulating shell made of ligands protecting the core. As necessary as the presence of the ligands was throughout the reaction as deleterious it becomes to charge carrier transport when

incorporated into the nanostructured bulk solid. In order to fabricate shape- and size-controlled nanostructured bulk solids with high electric conductivities it is mandatory to remove the ligands after the synthesis and before hot-pressing to pellets. Further, unprotected nanograins obtained after ligand removal possess very high surface energies and are prone to post-synthetic grain-growth during hot-pressing. Duration and temperature of the pressing procedure must therefore be kept to a minimum. In this respect, hot-pressing with the aid of a pulsed, high DC current, known as spark plasma sintering (SPS), is found to be an ideal technique. The sintering duration can be shortened to minutes and the overall temperature necessary for good compaction of the grains is usually significantly lower than with conventional, furnace driven systems. As an example for the potential of the bottom-up approach, we will present the synthesis and thermoelectric properties of colloidal bismuth telluride nanoparticles.

EXPERIMENT

Bismuth telluride nanoparticles were synthesized following a previously developed protocol [6]. The as-prepared, 1-dodecanethiol stabilized nanoparticles were precipitated with ethanol and the supernatant removed after centrifugation. The black precipitate was mixed with a large excess of oleic acid (~3 mL, 90 %, Aldrich) and allowed to stir overnight on which a black suspension was formed. The supernatant was removed after short centrifugation and fresh oleic acid was added on which the mixture was allowed to stir for several hours. The supernatant was removed again after centrifugation and it was washed three times with hexane (analytical grade, Aldrich). The precipitate was suspended in a solution of NH_3 in methanol (2 mL, 7 N, Aldrich). After stirring overnight, the supernatant was removed after centrifugation (4500 rpm, 5 min) and it was washed two times with fresh NH_3 in methanol followed by three washing steps with hexane. All solvents were removed and it was dried under vacuum overnight on which a fine black powder was obtained.

Typically, 100 mg of the powder kept under argon were loaded into a WC/Co die of 8.0 mm x 1.5 mm in area. The powder was pressed to a solid pellet of equal dimensions and approximately 1.5 mm in height by spark plasma sintering in a SPS-515 ET/M apparatus (Dr. Sinter®lab). For thermal conductivity measurements, 170 mg were loaded into a disk-shape die of 6 mm in diameter to obtain a tablet of bismuth telluride nanoparticles with 1.3 mm in height. On applying 340 MPa (for rectangular bars) or 530 MPa (for disks) pressure, the die containing the nanopowder was heated from 20 °C to 50 °C in 5.0 min with 10.0 min hold time by applying a DC current between 0 – 165 A and immediately allowed to cool down to room temperature. The obtained nanoparticle pellets were mechanically robust and silver-metallic in appearance.

DISCUSSION

Imaging of nanostructure

In Figure 1, transmission and scanning electron microscopy (TEM and SEM) is applied to investigate the size and shape of individual nanocrystals. The 1-dodecanethiol stabilized bismuth telluride nanoparticles are well separated by their ligand shell and readily soluble in a wide range of organic solvents ($CHCl_3$, toluene, hexanes, etc.). The narrow size distribution is the consequence of well controlled nucleation and growth stages during the reaction. The size of

nanocrystals can be controlled between 7 and 20 nm without significant broadening of size-distribution by changing the concentration of reactants. For a theoretical introduction the reader is referred to LaMer et al. [7] The shape of nanocrystals can be tuned from spheres to stars, platelets, and sheets by altering reaction conditions slightly (not shown here). Such a remarkable control over individual nanocrystals is unprecedented by top-down techniques and allows for exciting new possibilities to tune thermoelectric properties of these materials. For example, controlling the shape of bismuth telluride nanoparticles could be applied to benefit from the highly anisotropic, direction-dependent figure of merit [8]. Size-control allows studying the size effect on thermoelectric properties and utilizing recent theoretical predictions to improve the thermoelectric figure of merit [9]. A narrow size distribution is mandatory to enable efficient charge carrier transport between the nanograins and minimize charge carrier scattering [10].
All of the afore mentioned advantages depend crucially on the presence of stabilizing organic ligands. In their absence, shape control disappears, size distribution broadens dramatically, and the tuning possibilities are lost. To allow for high electric conductivities, organic ligands must not be incorporated into the nanostructured bulk solid. Our ligand removal procedure is simple, at low-cost, and highly efficient (see transport properties further down).
As visible in SEM imaging, careful choice of SPS parameters [6] allows compacting ligand-free nanoparticles to a dense pellet without significantly changing their size and shape. Relative density of typical pellets is 80 %.

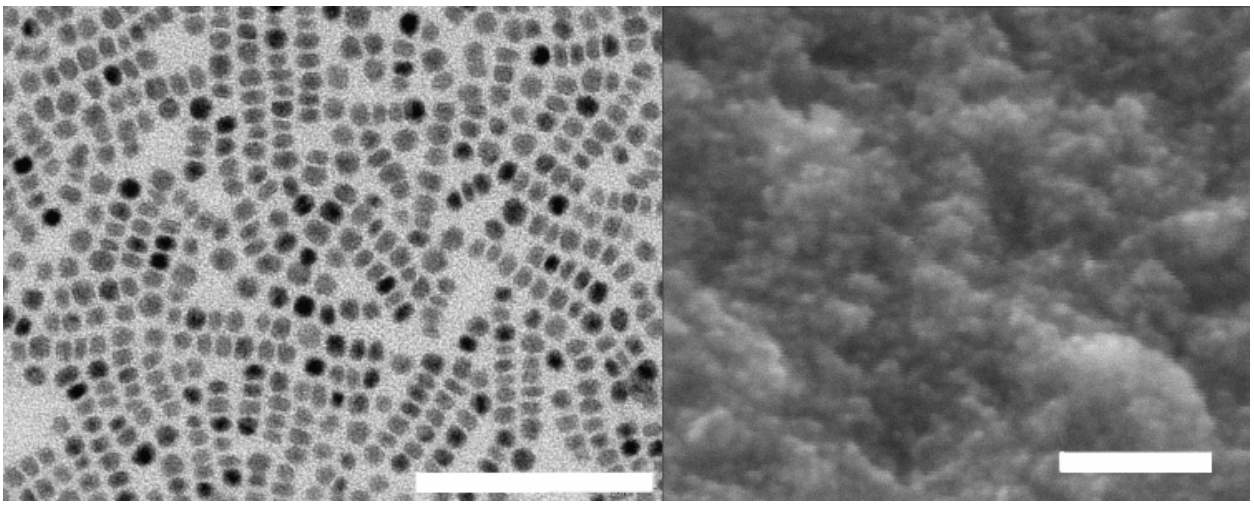

Figure 1: Imaging of nanostructures. (**Left**) TEM image of 1-dodecanethiol stabilized bismuth telluride nanoparticles on amorphous carbon substrate. (**Right**) SEM image of ligand-free, SPS compacted bismuth telluride nanoparticles. Scale bars correspond to 100 nm.

Charge carrier transport

Electric conductivity (σ) of nanostructured bulk bismuth telluride solids is only slightly decreased with respect to bulk samples (Figure 2, left). This is the result of efficient ligand removal and purification of the nanocrystalline powder. Unlike bulk Bi_2Te_3, σ has a positive dependence on temperature (T) around room temperature. We attribute this to the effect of grain boundary potential barrier scattering [11]: Due to crystal defects and dangling-bonds, each nanograin in the nanostructured sample possesses a large density of trap-states. Such trap-states immobilize charge carriers at the grain surface meanwhile charging it up. Charged surfaces provide a potential barrier (E_B) to charge carrier transport and lead to a changed $\sigma(T)$ according

to $\sigma(T) \sim T^{-1/2} \exp[-E_B/kT]$. Thus, for certain temperatures and magnitudes of E_B, $\sigma(T)$ can become positive regardless of its behavior in single crystals. We note that this shifts the maximum in the thermoelectric power factor to significantly higher temperatures as compared to bulk Bi_2Te_3.

At present, the thermopower (S) (Figure 2, right) is significantly decreased compared to bulk Bi_2Te_3. This is the result of a non-optimized chemical composition and is subject to future work under way. According to Inductively Coupled Plasma Optical Emission Spectroscopy, the present material is tellurium deficient and is better described by the formula $BiTe_{1+x}$ rather than Bi_2Te_3. Chemical composition is known to have a large impact on S in bismuth tellurides [12]. Crystal defects may play an additional role in reducing S [6].

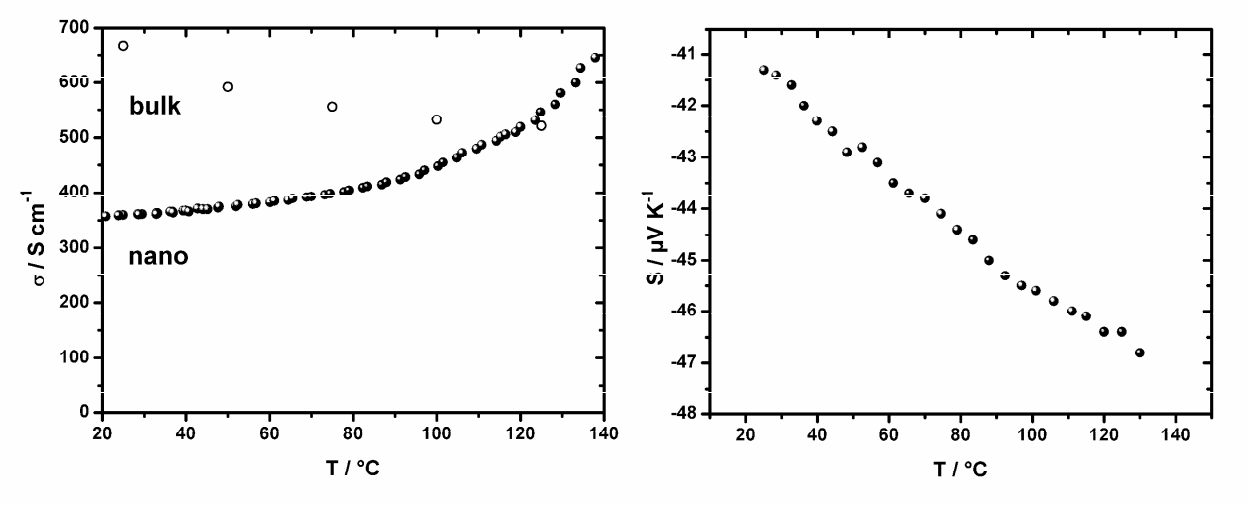

Figure 2: Charge carrier transport. (Left) Electric conductivity of nanostructured (full circles) versus bulk (open circles) bismuth telluride [13]. (**Right**) Thermopower of nanostructured bismuth telluride bulk solid.

Thermal transport

As displayed in Figure 3 (left), thermal transport (κ) is drastically inhibited in nanostructured bismuth telluride solids. This is attributed to a remarkable decrease in lattice thermal conductivity by as much as 80 % as compared to bulk bismuth telluride. To some degree, the low thermal conductivity is likely to be the result of porosity (P) in the sample. We account for this by applying a Maxwell-Eucken-type correction to derive the theoretical total thermal conductivity (κ_{corr}) of a sample with the same nanostructure but 100 % relative density by following $\kappa_{corr} = \kappa \cdot (1+P)/(1-P)$. As a verification of this correction we refer to Chiritescu et al. who calculated the thermal conductivity of nanostructured Bi_2Te_3 with an average grain size of 15 nm within the assumptions of the Debye-Callaway model [14]. Their room temperature value is almost identical with our porosity corrected value implying that the scattering effect of the nanostructure is fully operative. The additional decrease of 0.2 $W\,m^{-1}K^{-1}$ in κ beyond the Debye-Callaway predicted value is therefore due to porosity.

Another result of the nanostructure is a significantly increased specific heat capacity (C_P) as displayed in Figure 3 (right). The increase by roughly 30 % is typical for highly granular systems and can be attributed to the large percentage of surface atoms which possess different vibrational energies compared to atoms inside the crystal [15].

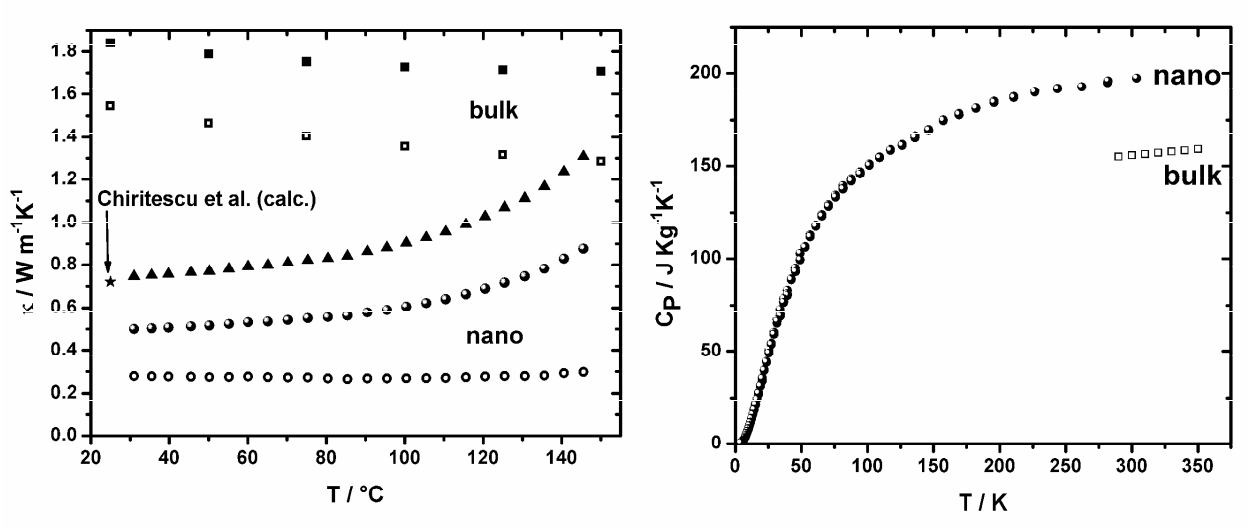

Figure 3: Thermal transport. (Left) Thermal conductivity of nanostructured (circles) versus bulk (squares) bismuth telluride [13]. Lattice thermal conductivities (open symbols) were calculated according to Wiedemann-Franz assuming $L = 2.0 \cdot 10^{-8}\ V^2\ K^{-2}$. A correction for porosity in the nanostructured sample was applied to display the thermal conductivity of a theoretical sample with 100 % relative density (triangles). A calculated value for nanostructured bulk Bi_2Te_3 of 15-nm grain size was included for comparison (stars) [14]. (**Right**) Specific heat of nanostructured (circles) versus bulk (squares) bismuth telluride [16].

RESULTS

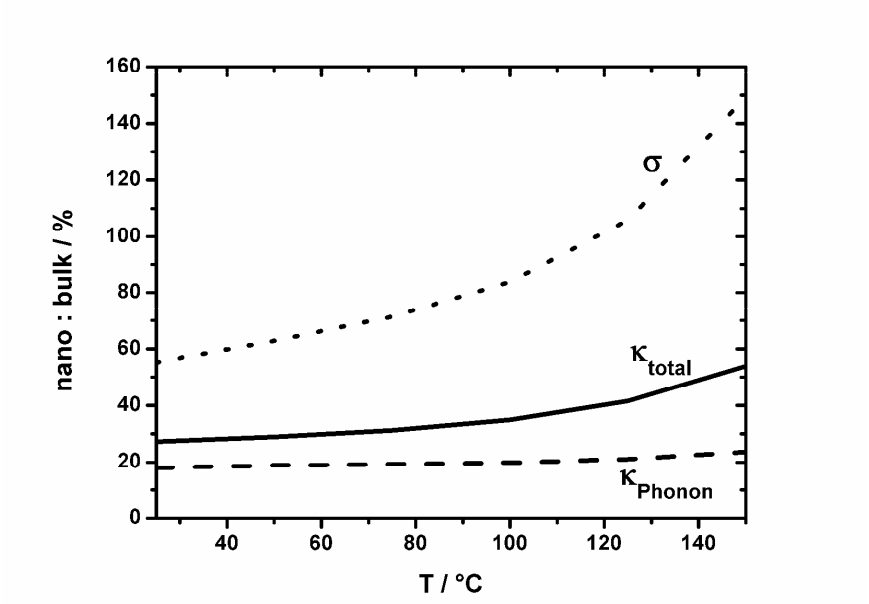

Figure 4: Relative transport properties. The effect of nanostructuring is investigated by plotting the ratio of electric conductivity (dotted), total thermal conductivity (solid) and lattice thermal conductivity (dashed) of nanostructured bismuth telluride divided by the values for bulk bismuth telluride [13] as a function of temperature.

To sum up the results of this work, we plot the relative transport properties in Figure 4 by dividing the individual property measured for nanostructured bismuth telluride by the same property reported for bulk samples. For the whole temperature range investigated, relative σ is significantly higher than relative κ, implying that phonons are scattered to a higher degree than

electrons. Thus, we have made a material with phonon-glass electron-crystal properties. Such materials have great potentials due lead to significantly enhanced ZT values. Due to the non-optimized chemical composition and the reduced thermopower, the current ZT is only about 0.1. Future work is under way to tune the thermopower towards the bulk value and benefit from the phonon-glass electron-crystal effect in this nanostructured material made by wet-chemistry.

ACKNOWLEDGMENTS

We thank Igor Veremchuk for performing additional SPS experiments, Klaus-Georg Reinsberg for ICP-OES analysis and gratefully acknowledge a PhD grant by the *Studienstiftung des deutschen Volkes*.

REFERENCES

1. B. Poudel, Q. Hao, Y. Ma, Y. Lan, A. Minnich, B. Yu, X. Yan, D. Wang, A. Muto, D. Vashaee, X. Chen, J. Liu, M. S. Dresselhaus, G. Chen, Z. Ren, *Science* **2008,** *320*, 634.
2. W. Z. Wang, B. Poudel, D. Z. Wang, Z. F. Ren, *Adv. Mater.* **2005**, 17, 2110.
3. J. Martin, G. S. Nolas, W. Zhang, L. Chen, *Appl. Phys. Lett.* **2007**, 90, 222112.
4. L. D. Hicks, M. S. Dresselhaus, *Phys. Rev. B* **1993,** 47**,** 12727
5. R. Y. Wang, J. P. Feser, J.-S. Lee, D. V. Talapin, R. Segalman, and A. Majumdar, *Nano lett.* **2008**, 8, 2283
6. M. Scheele, N. Oeschler, K. Meier, A. Kornowski, C. Klinke, and H. Weller, *Adv. Funct. Mater*. **2009**, 19 (21), 3476
7. V. K. LaMer and R. H. Dinegar, *J. Am. Chem. Soc.* **1950**, 72, 4847
8. J. P. Fleurial, L. Gailliard, R. Triboulet, H. Scherrer, and S. Scherrer, *J. Phys. Chem. Solids **1988***, 49, 1237
9. A. Popescu, L. M. Woods, J. Martin, and G. S. Nolas, *Phys. Rev. B* **2009**, 79, 205302
10. D. V. Talapin, J.-S. Lee, M. V. Kovalenko, and E. V. Shevchenko, *Chem. Rev.* **2010**, 110, 389
11. J. Martin, L. Wang, L. Chen, and G. S. Nolas, *Phys. Rev. B* **2009**, 79, 115311
12. J. W. G. Bos, H. W. Zandbergen, M.-H. Lee, N. P. Ong, and R. J. Cava, *Phys. Rev. B* **2007**, *75*, 195203
13. B.-L. Huang, M. Kaviany, *Phys Rev. B* **2008**, 77, 125209
14. C. Chiritescu, C. Mortensen, D. G. Cahill, D. Johnson, and P. Zschack, *J. Appl. Phys.* **2009**, 106, 073503
15. K. N. Shrivastava, *Nano lett.* **2002**, 2, 21
16. *Landholt-Bornstein*. O. Madelung, M. Schulz and H. Wiess. Berlin, Springer-Verlag. 17f: various (**1983**)